1   Title: Mexican blind cavefish use mouth suction to detect obstacles

2

3

4

5   Roi Holzman[1,2*], Shimrit Perkol-Finkel[3], Gregory Zilman[3]

6

7   [1] Department of Zoology, Faculty of Life Sciences, Tel Aviv University, Tel Aviv

8   69978, Israel

9   [2] The Inter-University Institute for Marine Sciences, POB 469, Eilat 88103, Israel

10   [3] School of Mechanical Engineering, Faculty of Engineering, Tel Aviv University,

11   Tel Aviv 69978, Israel

12   *Corresponding author

13

15

16

17

Abstract:

Fishes commonly use their lateral line system to detect moving bodies such as prey and predators. A remarkable case is the Mexican blind cavefish *Astyanax fasciatus* who evolved the capability to detect non-moving obstacles. The swimming body of *A. fasciatus* generates fluid disturbances, whose alteration by an obstacle can be sensed by the lateral line system. It is generally accepted that these alternations can provide information on the distance to the obstacle. We observed that *A. fasciatus* swimming in an unfamiliar environment open and close their mouths at high frequency (0.7-4.5 Hz) to generate suction flows. We hypothesized that repeated mouth opening generate a hydrodynamic velocity field, whose alterations by an obstacle induce pressure gradients in the neuromasts of the lateral line and corresponding strong lateral line stimuli. We observed that the frequency and rates of mouth opening events varied with the fish's distance to obstacles, a hallmark of pulse-based navigation mechanisms such as echolocation. We formulated a mathematical model of this hitherto unrecognized mechanism of obstacles detection and parameterized it experimentally. This model suggests that suction flows induce lateral line stimuli that are weakly dependent on the fish's speed and may be an order of magnitude stronger than the correspondent stimuli induced by the fish's gliding body. We illustrate that *A. fasciatus* can navigate non-visually using a combination of two deeply ancestral and highly conserved mechanisms of ray-finned fishes: the mechanisms of sensing water motion by the lateral line system and the mechanisms of generating water motion by mouth suction.

1 **Introduction**

2 The Mexican blind cavefish, *A. fasciatus* lost its eyes over the course of evolution

3 following multiple independent colonization events of underground caves. It is

4 nonetheless able to successfully avoid obstacles and navigate by utilizing hydrodynamic

5 cues created by its own motion (Dijkgraaf, 1933; Dijkgraaf, 1947; Dijkgraaf, 1963). A

6 moving fish creates hydrodynamic disturbances, namely fluid velocity $\mathbf{V}$ and pressure

7 fields p, which vary with the distance to an obstacle h. It has been hypothesized that to

8 form the hydrodynamic image of an obstacle, the fish performs mapping of the

9 hydrodynamic fields $\mathbf{M}(\mathbf{V}, p)$ into the distance to the obstacle (Campenhausen et al.,

10 1981; Dijkgraaf, 1933; Dijkgraaf, 1947; Dijkgraaf, 1963). In the scientific literature, the

11 gliding body of fish is considered as the only source of the hydrodynamic fields $(\mathbf{V}, p)$.

12   To perform this mapping, a fish has to sense the water motion and pressure

13 gradients. Like other ray-finned fishes, *A. fasciatus* can sense hydrodynamic disturbances

14 using its lateral line, a specialized system of mechanoreceptors located along the fish's

15 head and body (Bleckmann, 2007; Montgomery et al., 1995). The lateral line consists of

16 mechanoreceptors protruding from the skin of fish (superficial neuromasts) and

17 mechanoreceptors located in canals beneath the skin (canal neuromasts). Superficial

18 neuromasts measure the velocity of the flow very close to the skin, while canal

19 neuromasts measure the water pressure difference between adjacent pores in the canal

20 (Denton and Gray, 1983; Denton and Gray, 1988; Denton and Gray, 1989; Denton and

21 Gray, 1982; Kroese and Schellart, 1992). Although surface and canal neuromasts have

22 overlapping functions, blind cave fish can still locate objects even with disabled surface

23 neuromasts (Montgomery et al., 2001); whereas the ability of these fish to navigate with

1   disabled canal neuromasts is impaired or even lost (Abdel-Latif et al., 1990). In other

2   words, *A. fasciatus* is capable of navigating using mapping of pressure fields into the

3   distance to the obstacle.

4   Given that the pressure created by the motion of a body in fluid is proportional to

5   the body's square velocity, faster Mexican blind cavefish should detect an obstacle

6   sooner, and start the avoidance maneuver earlier, at a greater distance from the obstacle.

7   However, turning distances of *A. fasciatus* from a wall were uncorrelated with its

8   swimming speed U (Teyke, 1985; Windsor et al., 2008). The apparent disparity was

9   explained as a result of a fish's analysis of the relative, rather than the absolute,

10   magnitude of the pressure difference (Windsor et al., 2008). To the best of our

11   knowledge, alternative hydrodynamic mechanisms of obstacle detection, in which the

12   stimuli that trigger an obstacle-avoiding maneuver are weakly dependent on a fish's

13   speed, are currently unknown.

14   Virtually all fish use mouth suction, an evolutionarily conserved and deeply

15   ancestral method for prey capture and transport among teleosts (Lauder, 1980; Lauder,

16   1982; Lauder, 1985). To generate suction, fish rapidly open their mouth and expand their

17   buccal cavity, generating fast flows and steep pressure gradients that extend in front of

18   their mouths (Day et al., 2005; Day et al., 2007; Higham et al., 2006; Holzman et al.,

19   2008; Weihs, 1980). The mouth is then rapidly closed, and the time from the onset of

20   mouth opening until closing (hereafter "mouth opening event") takes 10-100 ms (Gibb

21   and Ferry-Graham, 2005). The same biomechanical mechanism is used to generate

22   respiratory flows, which are characterized by much slower flows and weak accelerations

23   (Brainerd and Ferry-Graham, 2006). In the context of suction feeding, it has been

1   previously shown that the fluid velocity and pressure fields change with the distance to a

2   wall (Nauwelaerts et al., 2007; Van Wassenbergh and Aerts, 2009) and thus can

3   potentially be utilized to detect obstacles using mapping of pressure to distance.

4   Our objective was to test whether mouth suction can be used as an additional

5   hydrodynamic mechanism of obstacle detection in Mexican blind cavefish. Specifically,

6   we ask whether mouth suction in *A. fasciatus* is performed in the absence of food and

7   whether the rate of mouth opening events is modulated as a function of the environment.

8   Lastly, we quantify the magnitude of the pressure gradient resulting from mouth suction

9   and compare it to that resulting from the translating body.

10

11   **Results**

12   *Experimental results*

13   Swimming freely in a familiar aquarium with no food and under well-ventilated

14   conditions (10.6-10.1 mg O_2 l^{-1}), *A. fasciatus* swam at an average speed of 0.75 bl s^{-1} ($\pm$

15   sd = 0.23; equivalent to 52.5 mm s^{-1} $\pm$ sd = 16.2). In the familiar environment, fish

16   opened and closed their mouths at a mean frequency of 0.2 $\pm$ sd = 0.23 Hz (n=30, range 0

17   - 1.08 Hz). After the obstacle in the tank where shifted to arbitrary locations, mouth

18   opening frequency increased significantly (Fig. 1; t-test, df = 60, $p<0.001$) by ~3.5 times

19   to a mean of 0.7 $\pm$ sd = 0.65 Hz (n=31, range 0 - 1.82 Hz) while swimming speed

20   decreased significantly (0.55 bl s^{-1} $\pm$ sd = 0.26; equivalent to 38.5 mm s^{-1} $\pm$ sd = 18.6; t-

21   test, df = 53, $p<0.006$). Within treatments, variance in mouth opening frequencies was not

22   significantly difference between individuals (Bartlett's test for homogeneity of variance,

23   df=2, p-value > 0.8).

1   In a separate set of experiments we focused on mouth opening events that

2   occurred when the fish swam towards the corner wall of the aquarium (Fig 2). FFT

3   analysis revealed that the frequency of mouth opening events at a distance of 110 - 0 mm

4   from the corner wall was 4.5 Hz (Figs. 2, 3A). The distribution of mouth-opening events

5   with respect to the distance from the corner, perpendicular to the direction of motion, was

6   significantly different from a uniform distribution (χ^2=61.31, Df=10, p<0.001). Mouth-

7   opening events were infrequent at a distance greater than 70 mm from the wall; their

8   frequency doubled were the fish were at a distance d of 70 > d > 10 mm; and was more

9   than 6 times higher at the last 10 mm from the corner (Fig. 3B).

10   High-speed videos taken during PIV experiments (1000 frames s^{-1}) indicate that

11   the maximal gape size G_{max} averaged 2.2 ± sd = 0.7 mm and time to peak mouth opening

12   T averaged 78 ± sd = 51 milliseconds (n = 14; Fig 4A; Table 1). The mouth returned to a

13   closed state after an additional 85 ± 61 milliseconds. High-speed Particle Image

14   Velocimetry (PIV; supplementary movie 2) indicated that peak flow speed at the center

15   of the mouth v_{max} averaged 66 ± sd = 22 mm s^{-1} (n = 14; range 22-110 mm s^{-1}; Fig. 4B;

16   Table 1)**.**

17

18   *A mathematical model of obstacle detection using mouth suction*

19   Fig. 6A illustrates that the pressure difference induced by the gliding body δp_B

20   grows monotonically with decreasing distance to the wall h, as expected (Milne-

21   Thomson, 1968) (see also similar results for a fish-like body of revolution (Windsor et

22   al., 2010)). The pressure difference induced by the gliding body δp_B is proportional to

1   U^2 (Fig 6 A-B), whereas the pressure difference induced by mouth opening $|\delta p_S|$ is

2   weakly dependent on a fish's speed.

3   Fig. 6A also illustrates that in each suction event the pressure difference induced by

4   mouth opening oscillates with the distance to the wall h and reaches two extrema

5   $\delta p_S(h_E)$ at two certain distances from the wall $h = h_E$. The absolute values of the

6   extrema also grow with decreasing distance to the wall. The larger of the two extrema

7   $\max |\delta p_S(h)| \equiv |\delta p_S(h_E)|$ may be two orders of magnitude higher than pressure difference

8   induced by the gliding body in the range of observed swimming speeds we observed (10

9   – 100 mm s^{-1}). In other words, the stimuli of canal neuromasts induced by mouth suction

10 may be much higher than those induced by a gliding body (Fig. 6A-B). It should be noted

11 however, that for high swimming velocities of order of 100 mm/s the two signals might

12 become of the same order of magnitude.

13   Additionally, in 14 mouth-opening events for which suction flow speed, swimming

14 speed and distance were available from PIV measurements (Table 1), the signals due to

15 mouth suction $|\delta p_S(h_E)|$ were ~50 fold stronger than those due to the gliding body

16 ($|\delta p_B(h_E)|$) (Fig. 6C; range 6-233, t-test, t=3.18, df=13, P<0.0071).

17

18 **Discussion**

19   In this paper we propose a new mechanism for non-visual navigation in *A.*

20 *fasciatus*. Mexican blind cavefish repeatedly generate mouth suction flows (Fig 1-3) to

21 produce pressure signals that can be used to detect non-moving obstacles (Fig 6). For the

22 swimming speeds and suction flows measured in our experiments for *A. fasciatus*

1   approaching to a wall, we calculated the pressure difference δp_S between two adjacent

2   canal pores (the received signal) due to mouth suction and the pressure difference δp_B

3   due to the gliding body. The results of our mathematical modeling suggest that δp_S may

4   be an order of magnitude stronger than δp_B (Fig 6C). The mouth suction signal depends

5   weakly on the speed of a fish but strongly on intensity of the suction flow. In contrast, the

6   body signal increases with the body velocity squared (U^2). Fig. 6 B depicts the ratio of

7   the signal induced by the mouth suction to the signal induced by the gliding body under

8   our parameters. As expected, this ratio depends on the fish swimming speed. For slow

9   swimming speeds (~2 cm/s) the body-induced signal may be much less effective than the

10   mouth suction signal. However, for faster swimming speeds (~10 cm/s) the body-induced

11   signal may be as effective as the mouth suction signal. Because the mouth suction signal

12   does not depend on the speed of a fish, it can be useful even when the fish is not moving,

13   whereas the body signal most effective during fast swimming. On the other hand, the

14   body signal is generated continuously whereas the mouth suction signal is intermittent.

15   A fish that uses its own gliding body for obstacle detection generates a monotonic

16   and slowly varying disturbance. Multiple mouth suction events generate oscillation

17   signals (Fig. 6A). Regardless of the mechanism that is used to generate pressure

18   gradients, the fish uses the same detector of varying pressure gradients, i.e. the lateral

19   line. However, canal neuromasts of *A. fasciatus* are relatively insensitive to slow flow

20   variations but sensitive to oscillating flows (Montgomery et al., 2009; Netten, 2006). Our

21   analysis of the dominant frequency of the mouth gape, the fluid velocity and the pressure

22   difference in the canal neuromasts induced by mouth suction is of order of 5-20 Hz (Fig

23   6; Table 1), which is close to the lower end of the sensitivity range of the canal

1   neuromasts [10-100 Hz, (Montgomery et al., 2009; Netten, 2006)]. Thus, the stronger

2   signal produced by mouth suction is also more likely to generate a strong neural response.

3   The gliding body and mouth suction generate water flows in opposite directions.

4   In the frame of reference of the fish, the flow velocity induced by the motion of the body

5   varies slowly in time, whereas that induced by the mouth suction varies rapidly. The

6   pressure gradients measured by the canal neuromasts is proportional to the flow

7   acceleration. Thus, even if the two peak velocities are of the same order of magnitude,

8   their accelerations are not. In this respect the two signals do not cancel each other.

9   Spatially, the suction flows generate radially symmetric flows around the fish's head,

10 which are measurable within a volume that is proportional to the cube of mouth diameter

11 (Day et al., 2005; Day et al., 2007). That flow field also extends ~1 mouth diameter

12 sideways to the head (Day et al., 2005; Ferry-Graham et al., 2003; Weihs, 1980). Thus,

13 even obstacles that are not directly in front of the mouth could elicit pressure gradient in a

14 neuromast. Clearly, this mechanism would not work for obstacles posterior to the head.

15   It follows from Euler equations (eq. 2) that the pressure created in inviscid fluid

16 by a moving body is proportional to the body's square velocity. Such correlation implies

17 an innate trade-off between signal strength and reaction time; speeding up increases the

18 signal but reduces reaction time to the obstacle. As previously noted, turning distances of

19 *A. fasciatus* from a wall were uncorrelated with its swimming speed U or with the fish's

20 size (Teyke, 1985; Windsor et al., 2008), and this pattern was explained as the fish's

21 analysis of the relative, rather than the absolute, magnitude of the pressure difference

22 between two adjacent pores (Windsor et al., 2008). It could also be that the fish prefers to

23 keep a close distance to the wall, therefore delaying the turn even though it is aware of

1 the wall in front of it. Here we illustrated that the pressure signal generated in the lateral

2 line by the mouth suction is weakly dependent on a fish's speed. Moreover, this

3 suggested mechanism can produce strong pressure signal even when the fish is not

4 moving. This novel result may provide an alternative explanation as to why the observed

5 initial distances of the avoidance maneuvers of *A. fasciatus*, do not depend on the speed

6 of the gliding body (Teyke, 1985; Windsor et al., 2008).

7   To detect underwater objects, cetaceans generate high frequency pressure

8 disturbances that propagate in water as acoustic waves whose length is much smaller than

9 the distance to a detected object (Friedlander, 1958). Using mouth suction, *A. fasciatus*

10 generates low frequency pressure oscillation whose wavelength is much larger than the

11 distance to the obstacle. In such a case the speed of sound can be considered infinite and

12 the water incompressible (Friedlander, 1958). Thus, the proposed mechanisms of obstacle

13 detection using mouth suction by transmitting oscillation signals is obviously not

14 acoustic. However, it shares certain features with echolocation. First, the high-frequency

15 suction flows generated by mouth suction in *A. fasciatus* can be seen as an active

16 emission of obstacle detection signals, one of the hallmarks of pulse-based navigation

17 mechanisms such as echolocation. Second, a salient feature of echolocation is that

18 animals increase the signal frequency in unfamiliar environments and when approaching

19 a target (Au, 1993; Busnel and Fish, 1980; Simmons et al., 1979; Yovel et al.,

20 2010). Such modulation of mouth-opening frequency was observed in our experiments

21 with Mexican blind cavefish (Fig. 1, 3B).

22   The suggested mechanism of obstacle detections in *A. fasciatus* is a combination

23 of two ubiquitous mechanisms of ray-finned fishes: the ability to perceive the fluid

1   motion using the lateral line system, and the ability to generate suction flow. The lateral

2   line system is an ancestral feature of teleosts (Philip et al., 2012), present also in

3   amphibians and Elasmobranchii (Dijkgraaf, 1963). Similarly, the ability to generate

4   mouth suction for prey capture, transport and respiration is ancestral to fishes, and is

5   shared by ray-finned fish, lobe-finned fish, amphibians and Elasmobranchs (Lauder,

6   1982; Lauder, 1985; Westneat, 2006). This constitutes a remarkable example of the

7   evolution of a novel mechanism from a combination of ancient mechanisms, originally

8   adopted for other functions. It also implies that this mechanism could be widespread,

9   potentially used by other blind fishes, deep-sea and nocturnal species.

10   The frequencies of mouth opening in familiar and unfamiliar environments (0.2-

11   0.7 Hz) are well within the range reported for mouth opening for respiration (Brainerd

12   and Ferry-Graham, 2006; Hughes, 1970; Hughes, 1960). However, our data suggests that

13   the increase in mouth opening frequency in unfamiliar environment is not due to

14   increased metabolic rates because in our experiments, fish swam slower in an unfamiliar

15   environment. Also, mouth-opening frequencies near the corner (4.5 Hz; Fig 3a) are much

16   higher than those observed during slow swimming in other species (Brainerd and Ferry-

17   Graham, 2006; Hughes, 1970; Hughes, 1960). Moreover, mouth opening events were X6

18   more likely to occur very close to the corner than at a distance of >7 cm away from it,

19   and it is difficult to explain this distribution based on metabolic demands. Lastly, *A.*

20   *fasciatus* was previously observed to swim in an unfamiliar environment at a speed that is

21   20-30% higher than that observed in a familiar environment (Burt de Perera, 2004;

22   Teyke, 1985). Based on studies in other fish species, such increase in swimming speed

23   should translate to a maximal increase of ~20% in mouth ventilation rate (and sometimes

1   even a decrease in that rate), compared to the x3.5 increase in our experiments (Altimiras

2   and Larsen, 2000; Clark and Seymour, 2006; Webb, 1971).

3   From a biomechanical perspective, mouth-opening events that generate

4   respiratory and suction feeding flows are very similar (Brainerd and Ferry-Graham, 2006;

5   Westneat, 2006). Both behaviors consist of buccal expansion to generate unidirectional

6   water flows through the mouth and out of the operculum. Hydrodynamically, both

7   behaviors generate unsteady flows that can be modeled as passive flow into an orifice.

8   Thus, both are "mouth suction" behaviors. Evolutionary, both behaviors are ancestral and

9   conserved across fishes, and have a shared biomechanical and neurological basis

10 (Brainerd and Ferry-Graham, 2006; Westneat, 2006). Therefore, we cannot determine

11 whether using mouth suction to detect obstacles evolved from respiratory or predatory

12 flows. However, the two behaviors (feeding and respiration) impose contrasting

13 functional demands. In respiratory flows, the efficiency of gas exchange is higher under

14 low flow speeds and weak accelerations (Brainerd and Ferry-Graham, 2006). To

15 effectively capture prey, fast flows and steep accelerations are beneficial (Holzman et al.,

16 2012; Holzman et al., 2007; Wainwright et al., 2007). Thus, the functional demands for

17 obstacle detection are more similar to those of suction feeding for prey capture. We do

18 not rule out that these flows are modified respiratory flows, and it may be that mouth

19 opening in blind Mexican cavefish is an intermediate between prey capture and

20 respiration.

21

22

23

1 **Methods**

2 *Filming of fish*

3 Fish were obtained from the pet trade and housed in 400×300×100 mm aquaria for 4-6

4 weeks before being transferred to the experimental aquaria. Holding aquaria contained a

5 sponge filter, with no additional obstacles. Fish were fed daily with commercial "Tetra

6 flakes". The experiments described below complied with IACUC approved guidelines for

7 the use and care of animals in research at Tel Aviv University, Israel.

8   To characterize mouth opening in *A. fasciatus*, fish (total lengths L=40-70 mm)

9 were introduced to an experimental aquarium (400×300×100 mm) and filmed using a pair

10 of high-speed (125 fps) synchronized digital video cameras (1280x1024 pixel CMOS,

11 Optronics GmBh, Germany) equipped with 60mm/f2.8 and 24mm/f1.8 lenses (Nikkor,

12 Japan). The first camera filmed the aquarium from above while the second had a lateral

13 view of one of the aquarium walls and corners (supplementary movie 1). Frame rate was

14 selected such that mouth opening is captured by >4 consecutive frames. The cameras

15 were set to cover an approximately 11x11 cm area of the aquarium, near one of the

16 corners. For the first camera, a grid was placed under the aquarium bottom to calibrate

17 the distances. For the second, a ruler was placed on the aquarium wall near the image

18 boundary. Fish were introduced into the aquarium, and immediately filmed when

19 swimming along one of the walls, towards the aquarium's corner. From the recorded

20 videos we selected sequences were the fish was continuously visible through its progress

21 towards the wall (5-20 s long, depending of the fish's swimming speed). For each

22 sequence analyzed, we recorded the time of each mouth opening event and the distance of

1 the fish from the aquarium wall in front of it. Overall, 123 mouth opening events were

2 analyzed.

3   To test whether the frequency of mouth opening in *A. fasciatus* is modulated in

4 unfamiliar environments, we allowed three *A. fasciatus* individuals (total lengths L=40-

5 70 mm) to acclimate for 48 hours in a 400×300×100 mm aquarium. The aquarium

6 contained five cylindrical obstacles of diameters 20-40 mm. Obstacles were made of

7 machined Polycarbonate, with a heavy steel base. Oxygen was monitored in the aquarium

8 using YSI ProODO oxygen optode (YSI, Yellow Springs, OH, USA). Following the 48

9 hours acclimating period, fish were filmed from the side at 60 fps for 15 minutes using a

10 commercial Sony HDR-CX550 camcorder (Sony, Japan). After filming, the obstacles

11 were shifted to arbitrary locations by moving a large magnet under the aquarium, and the

12 fish were filmed again. From the two filming periods (before and after moving the

13 obstacles) we selected short (2-10 sec) intervals in which a fish's mouth was continuously

14 observed in the field of view. The number of mouth opening events in the filming period

15 was quantified, and mouth-opening rate was calculated for each sequence. Overall, we

16 analyzed 30 sequences taken before obstacle shifting and 31 after. The duration of

17 filming was selected to ensure large enough sample size for statistical analysis.

18   We repeated this experiment, using a camera positioned above the aquarium, to

19 quantify the swimming speed of the fish in familiar and unfamiliar environments. Movies

20 were recorded using a GoPro Hero3 camera (San Mateo, USA) recording at 60 fps. We

21 randomly sampled 27 short clips (~1 s) during 5 min prior to obstacle shifting, and 27

22 short clips (~1 s) during 5 min immediately after obstacle shifting. We determined the

1 swimming speed in each clip by digitizing the fish's head and dividing the cumulative

2 swimming distance by the clip's duration.

3

4 *Particle Image Velocimetry (PIV)*

5   To characterize the flows produced in front of the mouth due to rapid mouth

6 opening, we used a flow visualization technique termed PIV. The details of this method

7 are described elsewhere (Holzman and Wainwright, 2009; Raffel et al., 1998) and are

8 discussed here only in brief. In general, this technique is used to obtain instantaneous

9 velocity measurements and derived properties in fluids. The fluid is seeded with small,

10 neutrally-buoyant particles and is illuminated such that particles are visible. The motion

11 of the particles is recorded using a high-speed camera, and is analyzed to calculate the

12 speed and direction of the flow in the field of view.

13   Fish were allowed to acclimate to their aquaria and the laser sheet described

14 below for a week prior to the PIV experiments. At the onset of each trial, the obstacles

15 were moved to arbitrary locations in the tank. We focused on an area of 5x5 cm near one

16 of the corners of the tank. Fish that swam voluntarily into this area were filmed and their

17 suction flows were analyzed. A Coherent Magnum II 665nm, 1500mw solid-state

18 continuous wave laser (fan angle of 10°; Coherent, Inc. Santa Clara, CA, USA) was used

19 to produce a laser sheet in the experimental aquarium. The laser sheet, ~5 cm wide and

20 0.1 mm thick was parallel to the long wall of the aquarium, and ~15 mm apart from it.

21 We focused on an area of approx 50 x 50 mm, bordering one of the aquarium's corners.

22 The plane of the sheet coincided with the centerline of fish that swam parallel to the wall.

23 To visualize the flow, the water was seeded with 12μm silver coated, hollow glass beads

1   with specific gravity of 1.05 (Potter industries Inc, Clrlstadt, NJ, USA). Fish were filmed

2   in lateral view using a high-speed digital video camera (1000 frames per second, Photron

3   SA-3, Photron inc, Japan) equipped with a 105 mm/f2.8 lens (Nikkor, Japan).

4   Additionally, a camcorder recording at 120 frames per second (Sony, Japan) captured

5   anterior views of the swimming fish, which were used to verify the orientation and

6   location of the fish within the laser sheet. Sequential images taken during mouth opening,

7   treated as image pairs, were analyzed using a cross-correlation algorithm in MatPIV

8   (http://www.math.uio.no/~jks/matpiv), an open software toolbox for PIV analysis in

9   MATLAB (MathWorks, Inc. MA, USA). Image pairs were analyzed using a windows

10   shifting technique, starting with 64x64 pixel interrogation areas and ending with 16x16

11   pixel areas (with 50% overlap) after 6 passes. The cross-correlation algorithm returned a

12   two-dimensional grid of vertical and horizontal velocities and signal-to-noise ratio (SNR)

13   for each image pair analyzed.

14   We extracted data on the magnitude of flow speed at the center of the mouth at each

15   time point. Velocity values with an SNR value lower than 2 were omitted (<10% of the

16   cases). We define peak flow speed as the maximum flow speed observed during a mouth

17   opening event. We analyzed only sequences in which the laser sheet intersected with the

18   mid-sagittal plane of the fish, as verified with the anterior view camera. In addition to the

19   calculation of the flow speed, we determined for each frame the longitudinal and

20   transverse coordinates of the anterior-most points on the fish's upper and lower jaws,

21   using MATLAB free package DLTdv5 (Hedrick, 2008). We used these landmarks to

22   calculate gape distance and the gape angle, the angle between the upper and lower jaw.

23   We also calculated the time to mouth opening as defined as the time it takes the fish to

1 open its mouth from 20% to 95% of the maximal gape observed during mouth opening

2 event (Holzman et al., 2008). Overall, we analyzed 14 mouth opening events for the 3

3 fish.

4

5 *Statistical analysis*

6 We used Bartlett's test for homogeneity of variance implemented in the software R

7 statistics (R Development Core Team, 2009) to test whether variation in mouth opening

8 frequencies was significantly different between individuals. A fast Fourier transform

9 (FFT) algorithm implemented in MATLAB (Mathworks, USA) was used on sequences of

10 repeated mouth opening to estimate the frequency of mouth opening events, and extract

11 the dominant frequency. A chi-square test was used to test whether the frequency of

12 mouth opening events was higher in different distances from the corner by comparing the

13 observed frequencies to a uniform distribution (same number of events in each distance

14 category). Unless otherwise stated, statistical tests were done in the software R statistics

15 (R Development Core Team, 2009). Throughout the text, means are shown with ±

16 standard deviation (sd).

17

18 *A mathematical model of obstacle detection using mouth suction*

19   The primary aim of our modeling is to clarify mathematically which of the physical

20 processes, the steadily gliding body of a fish or its unsteady mouth suction, generate

21 steeper pressure signals that can be sensed by the lateral line. Using the closed-form

22 expressions for the hydrodynamic field generated by an ellipsoid (Milne-Thomson,

23 1968), we calculated the pressure difference between two adjacent canal pores due to the

1   motion of the body. Using the closed-form expressions for the hydrodynamic field

2   generated by a disk of sinks (Tuck, 1970), we calculated the pressure difference between

3   two adjacent canal pores due to mouth suction. We then compared the magnitude of the

4   pressure gradients generated by the two mechanisms.

5   The input parameters used for our the mathematical modeling included fish length

6   L, peak mouth opening G_{max}, time to peak gape T and the peak velocity of the intake

7   flows with at the center of the mouth aperture v_{max}. We used the average values measured

8   during our PIV experiments (see "experimental results"). Four characteristic scales are

9   adopted here for the further asymptotic analysis: the length of fish L = 50 mm, the

10   minimal distance h_{min} = 5 mm at which Mexican blind fish starts the wall avoiding

11   maneuver (Windsor et al., 2008), the speed of fish U = 50 mm s^{-1} (Windsor et al., 2008),

12   and the time to mouth peak gape T = 0.1 s (see *Results*). For such problem parameters the

13   Reynolds numbers $Re = UL/v$ = 2500 is sufficiently low to assume a laminar motion of

14   the fluid around a fish's body and is sufficiently high to assume that a fish's body

15   boundary layers is thin, at least at its head (Vogel, 1994). According to the basic

16   assumptions of the boundary layer theory, the flow outside the boundary layer can be

17   considered as inviscid and irrotational (potential) (Schlichting, 1979). We also considered

18   the flow generated by the mouth aperture as inviscid and potential, because the distance

19   in front of the mouth aperture where the viscosity influences the velocity field due to

20   mouth suction [$\sqrt{vT} \approx 0.3$ mm (Tuck, 1970)] is much smaller than h_{min}.

21   Given that pores of canal neuromasts are spaced at relatively small intervals

22   δs with respect to the fish's length (Schemmel, 1967), the pressure difference in a

23   neuromast can be approximated as

18

1
$$\delta p = \delta \mathbf{s} \cdot \nabla p \qquad (1)$$

2

3 where $\delta \mathbf{s}$ is the vector connecting two adjacent pores and ∇p is the pressure gradient. In

4 the Earth-bound frame of reference the equation of motion of inviscid incompressible fluid

5 can be described by the Euler and continuity equations (Milne-Thomson, 1968).

6
$$\frac{\partial \mathbf{V}}{\partial t} + (\mathbf{V} \cdot \nabla)\mathbf{V} = -\frac{1}{\rho}\nabla p , \qquad (2)$$

7
$$\nabla \cdot \mathbf{V} = 0 , \qquad (3)$$

8 where ρ is the fluid density and t is the time. For potential flows the fluid velocity

9 vector $\mathbf{V}$ can be expressed as a gradient of a harmonic function (the velocity potential)

10 Φ, i.e.

11
$$\mathbf{V} = \nabla \Phi . \qquad (4)$$

12 Substituting (eq. 3) into (eq. 4) reduces the governing equation of the hydrodynamic

13 problem to the Laplace equation $\nabla^2 \Phi = 0$.

14   If a body moves in an unbounded fluid with constant velocity U then, in the frame

15 of reference attached to the body, the fluid motion is steady, and the local fluid

16 acceleration $\partial \mathbf{V} / \partial t$ on the right-hand side of (eq. 2) vanishes. If a body approaches a

17 wall, the geometry of the fluid domain varies in time, the fluid velocity becomes time

18 dependent, and the fluid acceleration in (eq. 2) becomes non-zero. It is important to note

19 that the fluid acceleration may become non-zero also due to the unsteady mouth suction.

20   Consider a fish moving with constant velocity U in the direction normal to an

21 infinite plane wall. Assume that the velocity field created by a fish in unbounded fluid is

22 known. To satisfy the conditions of impermeability on the wall exactly and on the fish

23 body approximately, we use the method of mirror images (Milne-Thomson, 1968), where

24 the hydrodynamic combination "fish-wall" is replaced by two identical fish ("$R + I$")

1   swimming in unbounded fluid along the same line with the same velocity U but in

2   opposite directions, where I is a mirror image of R with respect to the wall (Fig. 5). We

3   further assume that fish R is fixed in space and that the water moves with constant

4   velocity U directed from the fish's head to its tail; whereas the fish-image I moves with

5   velocity $2U$ with respect to R and with velocity U with respect to water. The moving fish

6   I generates water disturbances by its gliding body or by its mouth suction. These

7   disturbances create pressure gradients ∇p in the neuromasts of R, which are identical to

8   ∇p created in the same neuromasts by the wall in the combination "R+wall". Once ∇p is

9   defined, the pressure difference in two adjacent pores is also defined by (eq.2).

10   We further use two orthogonal coordinate systems, $O_1 xyz$ fixed in non-moving

11   fish R and $O\xi\eta\varsigma$ fixed in moving fish I ($O_1 x \parallel O\xi$, $O_1 y \parallel O\eta$ and $O_1 z \parallel O\zeta$. The axes

12   $O_1 x$ and $O\xi$ are collinear with $\boldsymbol{U}$. The relation between the two coordinate systems is

13   $\xi = x - 2Ut + h_0$, where h_0 is the distance between O and O_1 at the initial moment of

14   time $t = 0$. Assume that the fluid velocity potential φ of fluid disturbances generated by

15   the fish-image I in unbounded domain is known in the fixed in the image coordinate

16   system $O\xi\eta\zeta$. Using the principle of superposition of potentials the velocity potential of

17   the flow Φ can be represented in the fixed in space coordinate system $O_1 xyz$ as

18   $$\Phi(x, y, z) = Ux + \varphi(x - 2Ut, y, z, t), \tag{5}$$

19   where

20   $$\varphi = \varphi_B(x - 2Ut, y, z) + \varphi_S(x - 2Ut, y, z, t) \tag{6}$$

21   φ_B is the fluid velocity potential pertaining to the gliding body and φ_S to the mouth

22   suction. Assume that the potentials $\varphi_{B,S}$ are known. Assume also that fish is a slender and

1   streamlined body which generates in the fluid weak disturbances $\left|\nabla\varphi\right| << U$. Then,

2   substituting (eq. 6) into (eq.5), (eq.5) into (eq.4), (eq.4) into (eq.2) and neglecting higher

3   order terms $O\left(\left|\nabla\varphi_{B,S}\right|^2\right)$ in (eq. 2), we can decompose the pressure difference δp into

4   the pressure difference δp_B pertaining to a fish's gliding body and to that δp_S pertaining

5   to the mouth suction.

6   The only known exact solution of the Laplace equation for a three-dimensional

7   body moving in inviscid irrotational flow (potential) flow pertains to a rigid ellipsoid

8   (Lamb, 1932). To calculate the fluid disturbances generated by a fish's gliding body, we

9   replace its by a three dimensional ellipsoid $\xi^2/a^2 + \eta^2/b^2 + \zeta^2/c^2 = 1$ moving in

10   unbounded fluid with velocity U directed along the axis $O\xi$ (Supplementary figure 1).

11   The calculation of the fluid velocity potential and the corresponding fluid velocities that

12   result from the motion of an ellipsoid followed (Milne-Thomson, 1968) and is detailed in

13   the supplementary methods:

14   We consider the flow created by mouth suction as that created by a disk of sinks

15   of uniform density over the plane area contained by a circle $\eta^2 + \zeta^2 = r^2(t)$, $\xi = 0$

16   (Milne-Thomson, 1968) where the radius of the disk r varies in time as

17
$$r(t) = f(t)\frac{G_{max}}{2}, \tag{7}$$

18
$$G_{max} = G(t)\big|_{t=T} \tag{8}$$

19

20
$$f(t) = \begin{cases} (\tau e^{1-\tau})^\alpha & \text{for } \tau > 0 \\ 0 & \text{for } \tau \le 0 \end{cases}, \tag{9}$$

21

1    $\tau = (t - t_0)/T$, t_0 is the initial time of suction and $\alpha \approx 5$ is an experimental fitting

2   parameter. The total flow rate q through the circle can be estimated using PIV

3   measurements of the suction velocity $v_{max} f(t)$ in the center of the mouth aperture:

4    $$q = \pi v_{max} f(t) r^2 .$$ (10)

5   The fluid velocity on the central axis of the disk $O\xi$ ($\varpi = 0$) can be written as

6    $$u = \left.\frac{\partial \varphi}{\partial \xi}\right|_{\bar{r}=0} = v_{max} f(t) \left[1 - \frac{\xi^+}{\sqrt{1 + \xi^{+2}}} \right]$$ (11)

7   where $\xi^+ = \xi/r$ [(Lamb, 1932), see supplementary methods]. Equation (11) captures the

8   main spatial and temporal characteristic of the velocity field created by mouth suction

9   (Day et al., 2005; Day et al., 2007; Holzman et al., 2008; Muller et al., 1982)

10   (supplementary Figure 2). Once the fluid components of the disk-induced flow are

11   known, the disk induced velocity vector and its derivative with respect to time are also

12   defined.

13

1   *List of symbols*

2   *a ,b, c*-semi-axes of an equivalent ellipsoid

3   *G*- instantaneous mouth gape

4   G_{max} - peak mouth gape

5   *h*- the instantaneous distance from the plane of the mouth aperture to a plane wall

6   h_0 -the initial distance from the plane of the mouth aperture to a plane wall

7   h_E -distance from the plane of mouth to the wall when the suction induced stimulus

8   attains its maximum

9   I- symbolic notation of mirror image of fish

10   *L* -fish length

11   *p*-fluid pressure

12   *q*-flow rate through mouth aperture

13   R-symbolic notation of fish

14   *r*-equivalent radius of the mouth aperture

15   Re-the Reynolds number

16   *T*-time to mouth peak gape

17   *t*-time

18   t_0 -the initial time of water suction

19   *U*-fish speed

20   **V**-fluid velocity vector

21   v_{max} -maximum velocity of peak intake flows through the mouth aperture

22   *xyz*- coordinates of the fish-body-fixed orthogonal coordinate system O_1xyz

1 δs -distance between two adjacent pores

2 δp -pressure difference between two adjacent pores

3 ν -water kinematic viscosity

4 $\xi\eta\zeta$ - coordinates of the mirror-image-fixed orthogonal coordinate system $O\xi\eta\zeta$

5 ρ -water density

6 Φ -fluid velocity potential

7 φ - potential of fluid velocity disturbances

8 φ_B -potential of fish-body-generated fluid velocity disturbances

9 φ_S -potential of mouth-suction-generated fluid velocity disturbances

10 ∇ -differential operator of gradient

11

12

13

14

15

16

21

22

1   **References**
2
3   **Abdel-Latif, H., Hassan, E. S. and Von Campenhausen, C.** (1990). Sensory

4   performance of blind Mexican cave fish after destruction of the canal neuromasts.

5   *Naturwissenschafften* **67**, 237-239.

6   **Altimiras, J. and Larsen, E.** (2000). Non-invasive recording of heart rate and

7   ventilation rate in rainbow trout during rest and swimming. Fish go wireless! *Journal of*

8   *Fish Biology* **57**, 197-209.

9   **Au, W. W. L.** (1993). The sonar of dolphins: Springer.

10   **Bleckmann, H.** (2007). The Lateral Line System of Fish. In *Fish physiology*, vol.

11   Volume 25 eds. J. H. Toshiaki and S. Z. Barbara), pp. 411-453: Academic Press.

12   **Brainerd, E. L. and Ferry-Graham, L.** (2006). Mechanics of Respiratory

13   Pumps. In *Fish Physiology: Fish Biomechanics: Fish Biomechanics*, vol. 23 eds. R. E.

14   Shadwick and G. V. Lauder). UK: Elsevier.

15   **Burt de Perera, T.** (2004). Spatial parameters encoded in the spatial map of the

16   blind Mexican cave fish, Astyanax fasciatus. *Animal Behaviour* **68**, 291-295.

17   **Busnel, R. G. and Fish, J.** (1980). Animal sonar systems. New York: Plenum.

18   **Campenhausen, C., Riess, I. and Weissert, R.** (1981). Detection of stationary

19   objects by the blind Cave Fish *Anoptichthys jordani* (Characidae). *Journal of*

20   *Comparative Physiology A: Neuroethology, Sensory, Neural, and Behavioral Physiology*

21   **143**, 369-374.

22   **Clark, T. D. and Seymour, R. S.** (2006). Cardiorespiratory physiology and

23   swimming energetics of a high-energy-demand teleost, the yellowtail kingfish (Seriola

24   lalandi). *Journal of Experimental Biology* **209**, 3940-3951.

1   **Day, S. W., Higham, T. E., Cheer, A. Y. and Wainwright, P. C.** (2005). Spatial

2   and temporal patterns of water flow generated by suction-feeding bluegill sunfish

3   *Lepomis macrochirus* resolved by Particle Image Velocimetry. *Journal of Experimental*

4   *Biology* **208**, 2661-2671.

5   **Day, S. W., Higham, T. E. and Wainwright, P. C.** (2007). Time resolved

6   measurements of the flow generated by suction feeding fish. *Experiments in Fluids* **43**,

7   713-724.

8   **Denton, E. and Gray, J.** (1983). Mechanical factors in the excitation of clupeid

9   lateral lines. *Proceedings of the Royal Society of London. Series B. Biological Sciences*

10   **218**, 1-26.

11   **Denton, E. and Gray, J.** (1988). Mechanical factors in the excitation of the

12   lateral lines of fishes. In *Sensory biology of aquatic animals*, vol. 1 eds. J. Atema R. R.

13   Fay A. N. Popper and T. W. N.), pp. 595-617. New York: Springer-Verlag.

14   **Denton, E. and Gray, J.** (1989). Some observations on the forces acting on

15   neuromasts in fish lateral line canals. In *The Mechanosensory Lateral Line. Neurobiology*

16   *and Evolution*, eds. S. Coombs P. Gorner and H. Munz), pp. 239-246. New York:

17   Springer-Verlag.

18   **Denton, E. J. and Gray, J. A. B.** (1982). The rigidity of fish and patterns of

19   lateral line stimulation. *Nature* **297**, 679-681.

20   **Dijkgraaf, S.** (1933). Untersuchungen über die Funktion der Seitenorgane an

21   Fischen. *Journal of Comparative Physiology A: Neuroethology, Sensory, Neural, and*

22   *Behavioral Physiology* **20**, 162-214.

1   **Dijkgraaf, S.** (1947). Über die Reizung des Ferntastsinns bei Fischen und

2   Amphibien. *Cellular and Molecular Life Sciences* **3**, 206-208.

3   **Dijkgraaf, S.** (1963). The functioning and significance of the lateral-line organs.

4   *Biological Reviews* **38**, 51-105.

5   **Ferry-Graham, L. A., Wainwright, P. C. and Lauder, G. V.** (2003).

6   Quantification of flow during suction feeding in bluegill sunfish. *Zoology* **106**, 159-168.

7   **Friedlander, F. G.** (1958). Sound pulses. Cambridge: Cambridge University

8   Press

9   **Gibb, A. C. and Ferry-Graham, L.** (2005). Cranial movements during suction

10   feeding in teleost fishes: Are they modified to enhance suction production? *Zoology* **108**,

11   141-153.

12   **Hedrick, T. L.** (2008). Software techniques for two- and three-dimensional

13   kinematic measurements of biological and biomimetic systems. *Bioinspiration &*

14   *Biomimetics* **3**, 034001.

15   **Higham, T. E., Day, S. W. and Wainwright, P. C.** (2006). The pressures of

16   suction feeding: the relation between buccal pressure and induced fluid speed in

17   centrarchid fishes. *Journal of Experimental Biology* **209**, 3281-3287.

18   **Holzman, R., Collar, D. C., Day, S. W., Bishop, K. L. and Wainwright, P. C.**

19   (2008). Scaling of suction-induced flows in bluegill: morphological and kinematic

20   predictors for the ontogeny of feeding performance. *Journal of Experimental Biology*

21   **211**, 2658-2668.

1   **Holzman, R., Collar, D. C., Mehta, R. S. and Wainwright, P.** (2012). An

2   integrative modeling approach to elucidate suction feeding performance. *J Exp Biol* **215**,

3   1-13.

4   **Holzman, R., Day, S. W. and Wainwright, P. C.** (2007). Timing is everything:

5   coordination of strike kinematics affects the force exerted by suction feeding fish on

6   attached prey. *Journal of Experimental Biology* **210**, 3328-3336.

7   **Holzman, R. and Wainwright, P. C.** (2009). How to surprise a copepod: Strike

8   kinematics reduce hydrodynamic disturbance and increase stealth of suction-feeding fish

9   *Limnology and Oceanography* **54**, 2201-2212.

10   **Hughes, G.** (1970). A comparative approach to fish respiration. *Experientia* **26**,

11   113-122.

12   **Hughes, G. M.** (1960). A Comparative Study of Gill Ventilation in Marine

13   Teleosts. *Journal of Experimental Biology* **37**, 28-45.

14   **Kroese, A. B. and Schellart, N. A.** (1992). Velocity- and acceleration-sensitive

15   units in the trunk lateral line of the trout. *Journal of Neurophysiology* **68**, 2212-2221.

16   **Lamb, H.** (1932). Hydrodynamics. New York: Dover.

17   **Lauder, G. V.** (1980). Hydrodynamics of prey capture in teleost fishes. In

18   *Biofluid mechanics*, vol. II (ed. D. Schenck), pp. 161-181. New York: Plenum Press.

19   **Lauder, G. V.** (1982). Patterns of evolution in the feeding mechanism of

20   actinopterygian fishes. *American Zoologist* **22**, 275-285.

21   **Lauder, G. V.** (1985). Aquatic feeding in lower vertebrates. In *Functional

22   vertebrate morphology*, eds. M. Hildebrand D. M. Bramble K. F. Liem and D. B. Wake),

23   pp. 210–229. Cambridge, MA. : Harvard Univ. Press.

1   **Milne-Thomson, L. M.** (1968). Theoretical hydrodynamics. London: Macmillan.

2   **Montgomery, J., Coombs, S. and Halstead, M.** (1995). Biology of the

3   mechanosensory lateral line in fishes. *Reviews in Fish Biology and Fisheries* **5**, 399-416.

4   **Montgomery, J. C., Coombs, S. and Baker, C. F.** (2001). The Mechanosensory

5   Lateral Line System of the Hypogean form of *Astyanax Fasciatus*. *Environmental*

6   *Biology of Fishes* **62**, 87-96.

7   **Montgomery, J. C., Windsor, S. and Bassett, D.** (2009). Behavior and

8   physiology of mechanoreception: separating signal and noise. *Integrative Zoology* **4**, 3-

9   12.

10   **Muller, M., Osse, J. W. M. and Verhagen, J. H. G.** (1982). A quantitative

11   hydrodynamical model of suction feeding in fish. *Journal of Theoretical Biology* **95**, 49-

12   79.

13   **Nauwelaerts, S., Wilga, C., Sanford, C. and Lauder, G. V.** (2007).

14   Hydrodynamics of prey capture in sharks: effects of substrate. *Journal of the Royal*

15   *Society, Interface* **4**, 341-345.

16   **Netten, S.** (2006). Hydrodynamic detection by cupulae in a lateral line canal:

17   functional relations between physics and physiology. *Biological Cybernetics* **94**, 67-85.

18   **Philip, S., Machado, J. o. P., Maldonado, E., Vasconcelos, V. t., O'Brien, S. J.,**

19   **Johnson, W. E. and Antunes, A.** (2012). Fish Lateral Line Innovation: Insights into the

20   Evolutionary Genomic Dynamics of a Unique Mechanosensory Organ. *Molecular*

21   *biology and evolution* **29**, 3887-3898.

22   **R Development Core Team.** (2009). R: A language and environment for

23   statistical computing. . Vienna, Austria: R Foundation for Statistical Computing.

1   **Raffel, M., Willert, C. E. and Kompenhans, J.** (1998). Particle image

2   velocimetry: A practical guide. Berlin: Springer.

3   **Schemmel, C.** (1967). Vergleichende Untersuchungen an den Hautsinnesorganen

4   ober- und unterirdisch lebender Astyanax-Formen. *Zoomorphology* **61**, 255-316.

5   **Schlichting, H.** (1979). Boundary Layer Theory New York: McGraw-Hill.

6   **Simmons, J., Fenton, M. and O'Farrell, M.** (1979). Echolocation and pursuit of

7   prey by bats. *Science* **203**, 16-21.

8   **Teyke, T.** (1985). Collision with and avoidance of obstacles by blind cave fish

9   *Anoptichthys jordani* (Characidae). *Journal of Comparative Physiology A:*

10 *Neuroethology, Sensory, Neural, and Behavioral Physiology* **157**, 837-843.

11 **Tuck, E. O.** (1970). Unsteady flow of a viscous fluid from a source in a wall.

12 *Journal of Fluid Mechanics* **41**, 641-652.

13 **Van Wassenbergh, S. and Aerts, P.** (2009). Aquatic suction feeding dynamics:

14 insights from computational modelling. *Journal of The Royal Society Interface* **6**, 149-

15 158.

16 **Vogel, S.** (1994). Life in moving fluids. Princeton: Princeton University Press.

17 **Wainwright, P. C., Carroll, A. M., Collar, D. C., Day, S. W., Higham, T. E.**

18 **and Holzman, R.** (2007). Suction feeding mechanics, performance, and diversity in

19 fishes. *Integrative and Comparative Biology* **47**, 96-106.

20 **Webb, P. W.** (1971). The Swimming Energetics of Trout: I. Thrust and Power

21 Output at Cruising Speeds. *Journal of Experimental Biology* **55**, 489-520.

22 **Weihs, D.** (1980). Hydrodynamics of Suction Feeding of Fish in Motion. *Journal*

23 *of Fish Biology* **16**, 425-433.

1   **Westneat, M. W.** (2006). Skull biomechanics and suction feeding in fishes. In

2   *Fish Biomechanics*, eds. G. V. Lauder and R. E. Shadwick), pp. 29-75. San Diego:

3   Elsevier Academic Press.

4   **Windsor, S. P., Norris, S. E., Cameron, S. M., Mallinson, G. D. and**

5   **Montgomery, J. C.** (2010). The flow fields involved in hydrodynamic imaging by blind

6   Mexican cave fish (*Astyanax fasciatus*). Part I: open water and heading towards a wall.

7   *The Journal of Experimental Biology* **213**, 3819-3831.

8   **Windsor, S. P., Tan, D. and Montgomery, J. C.** (2008). Swimming kinematics

9   and hydrodynamic imaging in the blind Mexican cave fish (*Astyanax fasciatus*). *Journal*

10   *of Experimental Biology* **211**, 2950-2959.

11   **Yovel, Y., Falk, B., Moss, C. F. and Ulanovsky, N.** (2010). Optimal

12   Localization by Pointing Off Axis. *Science* **327**, 701-704.

13

14

1   Table 1: mouth opening and flow suction parameters obtained for 14 PIV measurements

2

G_{max} (mm)	T (s)	v_{max} (m/s)	h_0 (mm)	U (m/s)
1.6	0.025	0.066	13.1	0.054
2.4	0.059	0.109	8.1	0.054
2	0.045	0.066	1.6	0.020
1.68	0.035	0.089	11.6	0.015
1.34	0.038	0.066	19.8	0.041
1.71	0.075	0.057	22.2	0.049
2.28	0.11	0.056	20.5	0.059
1.38	0.095	0.06	14.5	0.012
2.3	0.062	0.077	25.1	0.053
3.29	0.25	0.085	11.2	0.010
3.8	0.09	0.04	13.2	0.012
1.6	0.02	0.022	8.3	0.012
2.2	0.11	0.05	6.4	0.012
3.15	0.091	0.091	10.3	0.044

3

4

1   **Figures**

2

3
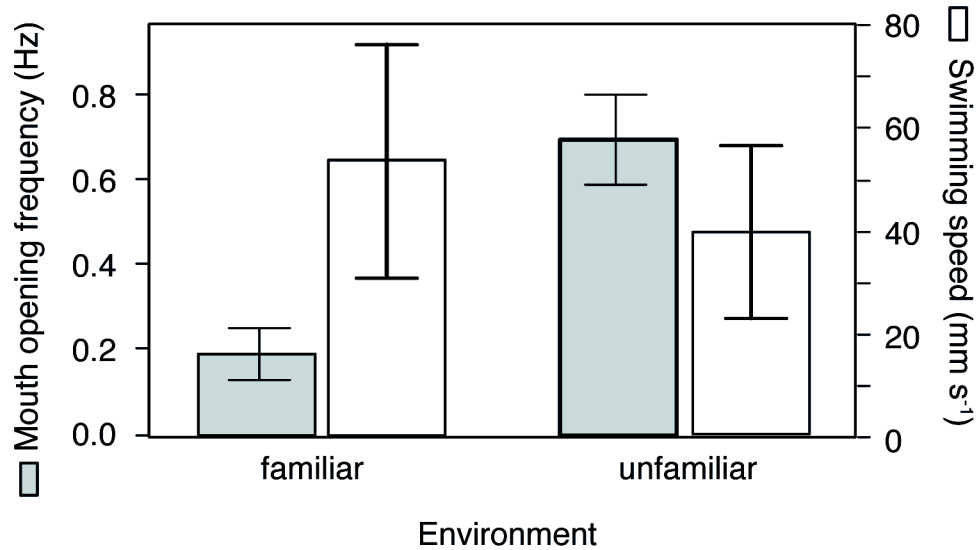
4   **Figure 1.** Mouth-opening frequency increases significantly in unfamiliar compared to

5   familiar environment (grey bars; t-test, $p<0.001$; $n=61$), while swimming speed was

6   lower in unfamiliar compared to familiar environment (white bars; t-test, $p<0.006$; $n=54$).

7   Fish were filmed in a familiar aquarium; then, obstacle positions were shifted arbitrarily
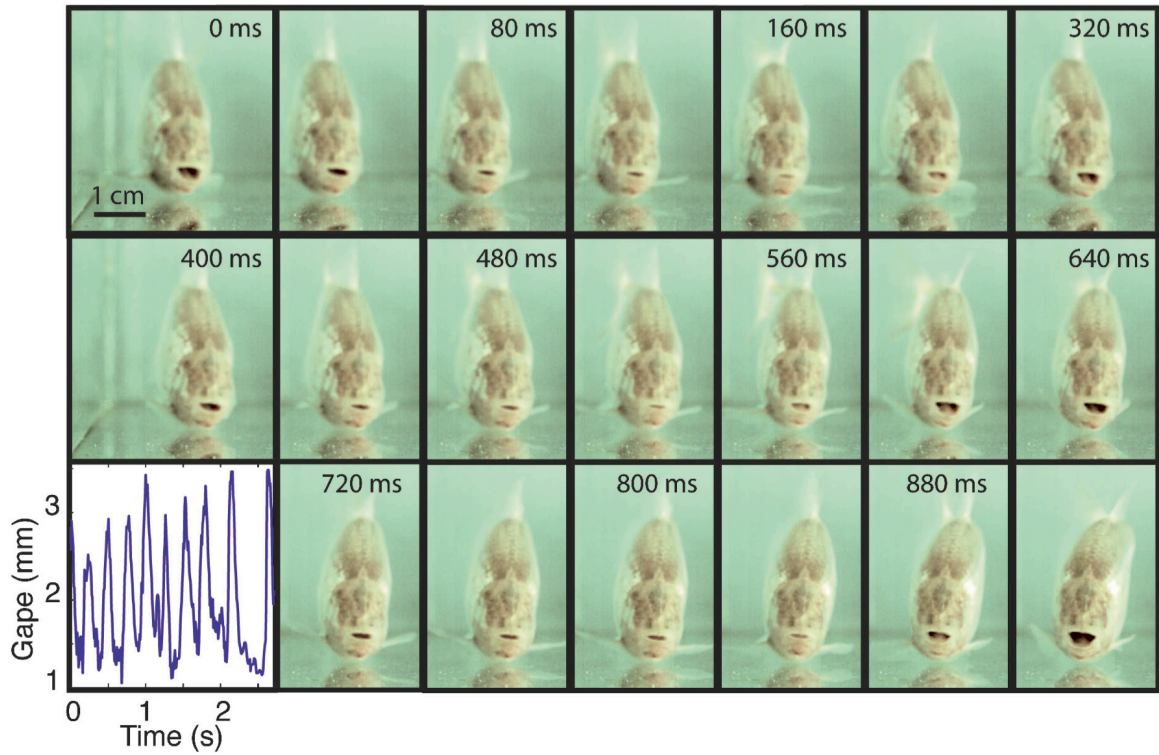
8   to create an unfamiliar environment.

9

10

Figure 2. Repeated mouth opening in *A. fasciatus* approaching a wall in an unfamiliar environment, digitized from supplementary movie 1. Original movie was filmed at 125 Hz. Image sequence depicts every 10th frame from the first frame of the movie. Bottom left panel is a frame-by-frame digitization of gape size through entire movie. The fish swims at a speed of 57 mm/s and starts turning at t = 2.75 s.
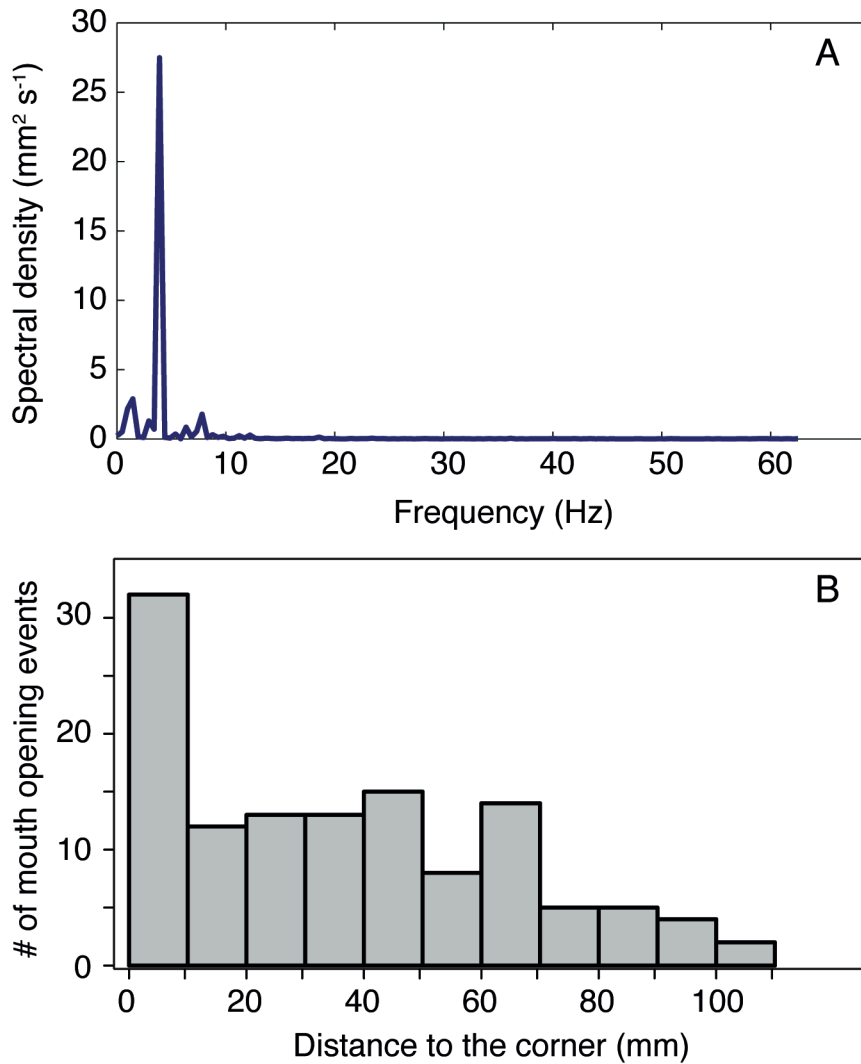
1

2 **Figure 3.** A) FFT analysis of mouth opening events, recorded when the fish swam

3 towards the corner wall of the aquarium. Data is from supplementary movie 1, which

4 captured mouth-opening events at a distance of 110 - 0 mm from the corner wall. B)

5 Frequency distribution of 123 mouth-opening events increased as a function of the

6 distance to the wall of the corner. Fish in B were filmed swimming towards the corner in

7 an unfamiliar environment at 125 frames s[-1]. The field of view started at a distance of

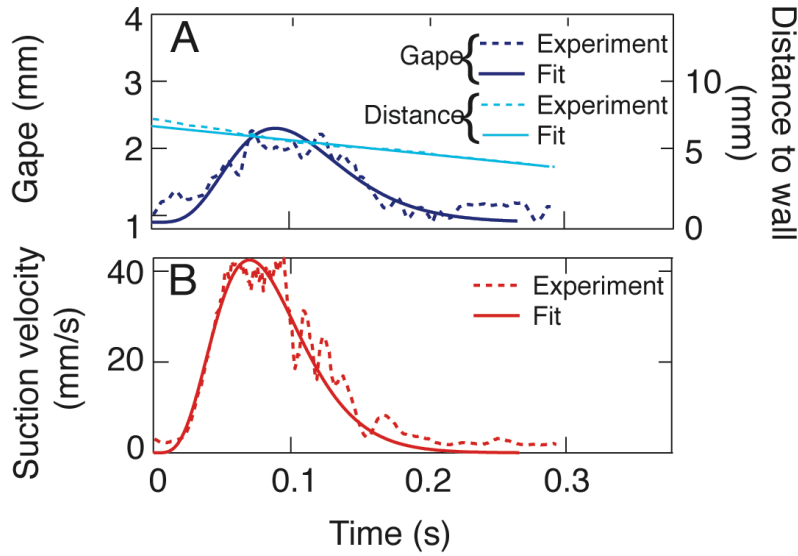8 ~110 mm from the corner. Distances from the wall are binned by 10 mm increments.

9

1

2

3   **Figure 4.** (A) A mouth-opening event from PIV experiments. The fish glides

4   forward at a speed of U=0.012 m s^{-1} when the mouth opens. (B) Water suction velocity in

5   the center of the mouth aperture measured using PIV. The observed gape size and suction

6   velocity in the center of the mouth aperture were fitted with a continuous function

7    $A_{max}f(t)$, where A_{max} denotes or G_{max} or v_{max}, and $f(t)$ is a continuous function

8   depending on time t (Muller et al., 1982); Supplementary methods).
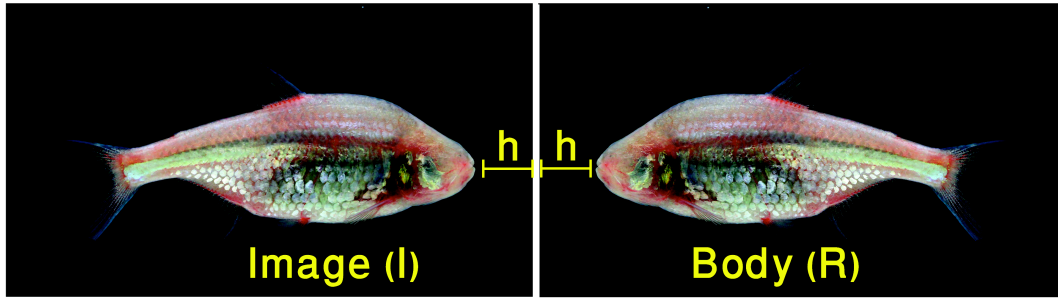
9

10

11

12

1

2

3

4 **Figure 5.** The method of hydrodynamic images. In the frame of reference attached to a

5 wall, fish (R) moves with speed U towards the wall bounding the right half-space. Fish

6 (I), a mirror image of (R) with respect to the wall, moves with the same speed U but in

7 the opposite direction. Due to symmetry, the fluid velocity normal to the plane that

8 separates the two fish is zero. Fish (I) induces in the neuromast fish (R) the same stimuli

9 that are induced by the wall.

10

11

12
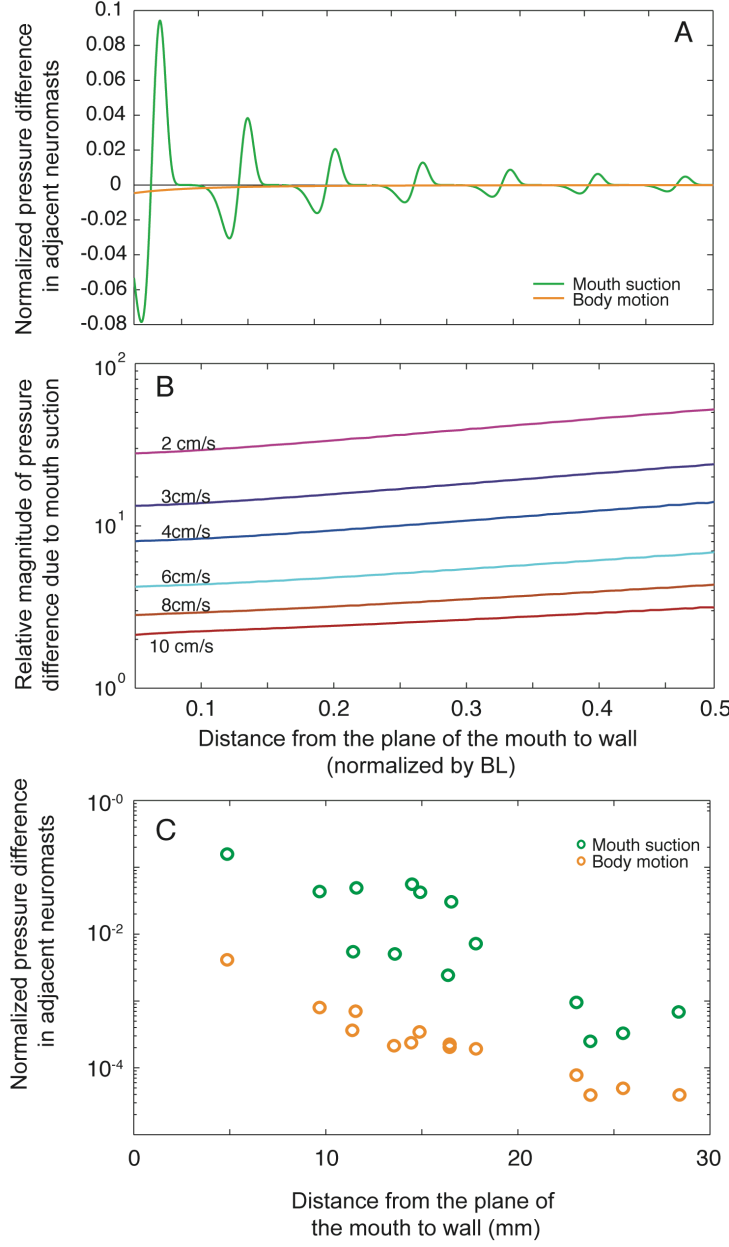
1

2 **Figure 6.** Pressure difference in adjacent pores as a function of the distance from the

3 mouth aperture to the wall. A) Simulated pressure differences $\delta p_B(h)$ and $\delta p_S(h)$ are

4 normalized with ρU^2. B) The simulated ratio $[(|\delta p_B| + |\delta p_S|)/|\delta p_B|]$ calculated for

5 $h = h_E$ and plotted for different swimming speeds U. In A-B the following parameters are

6 adopted: fish length $L = 5\,\text{cm}$, time to mouth-opening peak gape $T = 0.078\,\text{s}$, suction

1   fluid velocity v_{max} = 0.068 m/s, maximum mouth gape G_{max} = 2.5 mm. The pressure

2   gradient was calculated for a neuromast located at a distance of $0.1L$ from the plane of

3   mouth, and the distance between two adjacent pores was $\delta s = 0.02L$. C) Simulated

4   values of $\left| \delta p_B(h_E) \right|$ and $\left| \delta p_S(h_B) \right|$ for 14 mouth-opening events with PIV data are given

5   in Table 1.

6

7